

Identifications and spectroscopy of Gigahertz Peaked Spectrum sources. II.

W.H. de Vries^{1,2}, C.P. O’Dea², P.D. Barthel¹, and D.J. Thompson³

¹ Kapteyn Astronomical Institute, P.O. Box 800, NL-9700 AV Groningen, The Netherlands

² Space Telescope Science Institute, 3700 San Martin Drive, Baltimore, MD 21218, U.S.A.

³ California Institute of Technology, mailcode 320-47, Pasadena, CA 91125, U.S.A.

Received November 17, 1999; accepted January 11, 2000

Abstract. We present deep optical and near-infrared imaging as well as optical spectroscopy of as yet unclassified hosts of Gigahertz Peaked Spectrum (GPS) radio sources. Identifications were obtained for 14 objects, several of which are new. Spectroscopic follow-up yielded redshift information on 7 GPS objects. The remaining 18 objects of our sample without redshifts await spectroscopy with 8 m class facilities.

Key words: galaxies: active — galaxies: distances and redshifts — (galaxies:) quasars: emission lines

1. Introduction

Recent work has identified the GHz Peaked Spectrum (GPS) radio sources as the most likely candidates for the progenitors of the large scale powerful radio sources (e.g., Fanti et al. 1995; Readhead et al. 1996a,b; O’Dea & Baum 1997). The GPS sources are powerful but compact radio sources whose spectra are generally simple and convex with peaks near 1 GHz (O’Dea et al. 1991; De Vries et al. 1997; for a review see O’Dea 1998) and are entirely contained within the extent of the narrow line region (≤ 1 kpc). O’Dea (1998) estimates up to 10% of the sources listed in high frequency selected samples are GPS, underlining their relative large abundance. Still their relation to the large scale sources is not clear. It is fairly well established now that the extended radio galaxies and quasars should be unified with the compact, core dominated quasars and BL Lac objects through the combined effects of radio jet orientation and anisotropic obscuration (e.g., Urry & Padovani 1995). These objects are considered mature, well-developed radio sources. GPS objects, however, are proposed to be young radio sources which

will evolve into the 10 — 100 kpc scale radio sources. Constraints on numbers vs. linear size are consistent with simple models in which these sources propagate from the ~ 100 pc to Mpc scales at roughly constant velocity through an ambient medium with a density profile $\rho(R) \propto R^{-2}$, while the sources decline in radio luminosity as $L_{\text{rad}} \propto R^{-0.5}$ (Fanti et al. 1995; O’Dea & Baum 1997; Readhead et al. 1996b; De Young 1997; Begelman 1998). In addition, our multi-color optical (O’Dea et al. 1996) as well as near-IR imaging (De Vries et al. 1998a, 1998b; De Vries 1999) has shown that host galaxy colors of nearby GPS objects are indeed consistent with non- or passively evolving ellipticals, with absolute magnitudes somewhat fainter than brightest cluster members, similar to the hosts of intermediate sized and large radio source classes. Similar conclusions have been reached by Snellen et al. (1996). Determination of the rest-frame broad-band colors (which requires redshift information) in connection with stellar synthesis modeling has proven essential for these investigations.

GPS sources have been identified with both galaxies and quasars. Whereas almost all of the GPS quasars have been identified and spectrally investigated, the GPS galaxy spectral coverage is far less complete. The optically faint end of our GPS sample (O’Dea et al. 1991), combined with the unidentified part of this list, form a considerable fraction ($\sim 20\%$) of the total GPS galaxy population. In a previous paper (De Vries et al. 1995, hereafter Paper I), we reported on identification and spectroscopic work using 2 m class telescopes. Here we present our subsequent efforts on 4 m class instruments, to which we add a small amount of near-IR imaging data from the 10 m Keck-I telescope. While the imaging part of this program was fairly successful in identifying optical counterparts of the radio sources, spectroscopy of these objects proved often to be severely photon limited. Therefore, in order to complete the optical and spectroscopic content of the optically faint

part of our sample, we need to use 8 m class telescopes. In a further paper, we will report on our upcoming Very Large Telescope (VLT) results. This push towards higher redshifts and consequent enlargement of the GPS redshift baseline will improve our understanding of both the radio source and cosmological evolution of powerful radio sources (e.g. De Vries et al. 1998b; De Vries 1999).

2. Sample selection, observations, and data reduction

We selected 15 sources from the O’Dea et al. (1991) working list of powerful GPS sources, with either an “EF” or undetermined identification, or without a proper redshift determination. To this sample were added several GPS objects from various sources in the literature. Taken from White (1992): 0316+161, 0437–454, 0507+179, 1540–077, 1648+015, and 1815–553; and from O’Dea et al. (1990): 1045+019. The source 1245+676 is an extended radio source with a GPS core. Work on this source is in progress by De Bruyn et al. Furthermore, the spectra of 1848+283 and 2050+364, while observed quite some time ago, are presented here for the first time. Table 1 summarizes the objects, their origin, and the observational details.

In addition, we present 5 minute *K*-band images taken with the Keck-I telescope of 1942+722, 2121–014, 2128+048, and 2322–040.

2.1. Observations

The first observations of this program were taken at the ESO 2.2 m telescope at La Silla (Chile) in November 1993. This telescope was equipped with an imaging spectrograph (EFOSC2), so immediately after a successful identification a spectrum can be taken, making this setup ideal for our program. Based on our experience from this run in 1993 (Paper I), it became clear large apertures and long exposures are needed to obtain redshifts for most of these faint objects. We obtained imaging and spectroscopy of the southern part of the sample using EFOSC1 on the ESO 3.6 m, and spectroscopy of the northern objects using CRYOCAM on the 4 m Mayall telescope at Kitt Peak (U.S.A.). A few additional observations were obtained at Keck and Lick observatories. The next couple of paragraphs describe the instrumental setups at the respective observing runs.

The Kitt Peak run of January 1996 was on the 4 m telescope with the CRYOCAM instrument. We used grism 810 in combination with the Schott GG 455 blocking filter to suppress the 2nd order below 9000 Å. The unresolved lines had a FWHM of ~ 30 Å, or equivalently, a 1500 km s^{-1} resolution. The spatial resolution of the CRYOCAM is 0.84 arcsecond/pixel, and we used a $2''.5$ wide slit. The typical seeing through the slit was on the same order, so a narrower slit would have resulted in light loss.

Our March 1996 run was on the ESO 3.6 m telescope in La Silla. Like the 2.2 m, this telescope was equipped with an imaging spectrograph, EFOSC1, an instrument similar to EFOSC2. The installed chip was ESO CCD #26, which has a 0.61 arcsecond/pixel spatial scale. In combination with the R300 low dispersion grism, this setup resulted in a spectral resolution of ~ 20 Å (FWHM), quite comparable to both previous runs. Seeing permitting, we used the $1''.5$ slit, but on some occasions we had to use the $2''$ slit. The seeing hovered around the $1''.2$ mark on both nights.

Observations of 1848+283 date back to July 1990, and were taken at La Palma’s INT telescope in service mode. The telescope at the time was equipped with the Faint Object Spectrograph which simultaneously dispersed the wavelength ranges of 5000 – 10000 Å in first order and 3000 – 6000 Å in second order. This setup resulted in resolutions of 20 Å for the red and 10 Å for the blue arm of the spectrograph respectively. The spectrum of the source 2050+364 was taken in October 1991 at the 3 m Lick telescope. The resolution, as measured from sky-lines, was around 15 Å.

The *K*-band images were obtained on July 6 1998 with the NIRC instrument on the Keck-I telescope, the near-infrared camera (Matthews & Soifer 1994). NIRC re-images the telescope focal plane onto a 256^2 InSb detector at $0''.15$ per pixel, giving a field of view of $38''.4$ square. The night was photometric, with a seeing of $0''.4$ FWHM. Five dithered 60-second images were obtained on each field.

2.2. Data reduction

Images were reduced within IRAF¹. Standard optical reduction procedures were applied to remove the detector signature. Astrometry was performed using HST guide stars, of which typically 2–3 could be identified in the source fields. We used the APPHOT package, available in IRAF, for the *V*, *R*, *I*, and *K*-band photometry.

Spectral reduction was done with the NOAO longslit reduction package in IRAF. He-Ar reference spectra, plus observations of several standard stars were used to perform the wavelength and flux calibrations.

¹ Maintained by the National Optical Astronomy Observatories (NOAO) in Tucson, Arizona. NOAO is operated by the Association of Universities for Research in Astronomy (AURA), under cooperative agreement with the National Science Foundation.

Table 1. Source list and observations

Name	Radio position (2000.0)		1 σ err (") ^a	ref	date	Imaging		Spectra	Sample ^b
	RA	DEC				exp (s)	ID	exp (s)	
0018+729	00 21 27.38	73 12 41.9	0.03	pa	Jan. 96	—	G	3600	O
0159+839	02 07 14.19	84 11 18.7	2.0	sp	Jan. 96	—	Q?	1800	O
0316+161	03 18 57.76	16 28 32.3	2.0	wr	Jan. 96	—	G	3600	W
0437-454	04 39 00.85	-45 22 22.4	0.02	ma	Mar. 96	300	G	1800	W
0500+019 ^c	05 03 21.18	02 03 04.5	0.05	pe	Nov. 93	1200	G	3600	O
0507+179	05 10 02.37	18 00 41.6	0.02	jo	Jan. 96	—	Q?	3600	W
0554-026	05 56 52.62	-02 41 04.5	1.4	me	Jan. 96	—	G	1800	O
0602+780	06 10 24.63	78 01 34.9	2.0	sp	Jan. 96	—	G	3600	O
0703+468	07 06 48.04	46 47 56.2	2.0	do	Jan. 96	—	G	3600	O
0742+103	07 45 33.06	10 11 12.7	0.05	pe	Mar. 96	2400	G	—	O
0802+212	08 05 38.46	21 06 51.4	2.4	do	Mar. 96	600	G	3600	O
0904+039	09 06 41.05	03 42 41.5	1.5	me	Mar. 96	600	G	—	O
0914+114	09 17 16.39	11 13 36.5	2.0	do	Jan. 96	—	G	3600	O
0941-080	09 43 36.90	-08 19 30.9	0.4	wr	Jan. 96	—	G	1800	O
1045+019	10 48 22.84	01 41 47.7	2.0	do	Mar. 96	600	EF	—	O2
1245+676	12 47 33.33	67 23 16.5	0.03	pa	Jan. 96	—	G	1800	O
1433-040	14 35 40.05	-04 14 56.1	1.2	do	Mar. 96	300	G	3000	O
1540-077	15 43 01.69	-07 57 06.8	2.0	wr	Mar. 96	120	G	3000	W
1543+005	15 46 09.58	00 26 24.8	0.4	wr	Jan. 96	—	G	1800	O
1601-222	16 04 01.69	-22 23 41.5	1.3	wr	Mar. 96	240	G	1800	O
1648+015	16 51 03.68	01 29 23.8	0.4	wr	Mar. 96	300	G	3000	W
1732+094	17 34 58.37	09 26 58.2	0.4	dr	Mar. 96	300	G	1500	O
1815-553	18 19 45.40	-55 21 20.8	0.02	jo	Mar. 96	240	G	2400	W
1843+356	18 45 35.11	35 41 16.7	0.03	pa	Jul. 90	—	G	900	O
1848+283	18 50 27.52	28 25 13.1	0.05	pe	Jul. 90	—	Q	900	O
1942+772	19 41 26.87	72 21 43.7	0.4	sn	Jun. 98	300	G	—	S
2050+364	20 52 52.06	36 35 35.3	0.03	pa	Oct. 91	—	G	2400	O
2121-014	21 23 39.17	-01 12 33.9	1.4	me	Jun. 98	300	G	—	O
2128+048	21 30 32.88	05 02 17.5	0.02	jo	Jun. 98	300	G	—	O
2322-040	23 25 10.21	-03 44 46.7	1.4	sp	Jun. 98	300	G	—	O

^a Error in the radio position. To this error one has to add the optical accuracy ($0''.5 - 0''.7$) in quadrature to obtain σ_α^2 and σ_δ^2 of Eq. (1).

^b Taken from original sample of: O = O'Dea et al. (1991), O2 = O'Dea et al. (1990), S = Snellen et al. (1998a), and W = White (1992).

^c Source is part of the Paper I sample, and is only included again because of the discussion in Sect. 4.

REFERENCES — (do) Douglas et al. 1996; (dr) Drinkwater et al. 1997; (jo) Johnston et al. 1995; (ma) Ma et al. 1998; (me) McEwan et al. 1975; (pa) Patnaik et al. 1992; (pe) Perley 1982; (sn) Snellen et al. 1998b; (sp) Spoelstra et al. 1985; (wr) Wright & Otrupcek 1990.

3. Results

3.1. Identifications

Similar to the procedure outlined in Paper I, we used the likelihood ratio

$$R = \sqrt{\frac{\Delta\alpha^2}{\sigma_\alpha^2} + \frac{\Delta\delta^2}{\sigma_\delta^2}} \quad (1)$$

as described by De Ruiter et al. (1977) to quantify the correctness of a particular identification. $\Delta\alpha$ and $\Delta\delta$ are measured offsets in RA and Dec between the optical and radio positions, σ_α^2 and σ_δ^2 are the sums of the squared 1σ errors in the optical and radio positions. Note that in most cases the radio accuracy is much higher than in the

optical (cf. Col. 4 in Table 1), so σ_α^2 and σ_δ^2 are dominated by the optical error in these cases. We estimate our optical accuracy to be $0.5''$ as in all cases we were able to identify HST guide stars within the field of view. An R -value less than three indicates a chance less than 1% to miss a true identification (assuming that the possible counterpart is the object closest to the radio position). The probability that a true optical counterpart has an R -value larger than some R_0 is given by $P(R > R_0) = e^{-R_0^2/2}$. Most of our identifications have R -values smaller than 2, and can be assumed correct. Besides, some of the higher R -values, for instance in the case of 1601-222 or 1648+015, do not necessarily indicate a misidentification. Their high R -value may be due to overestimates of the accuracy, which will

artificially inflate the R -value. The identification results are listed in Table 2, and finding charts for the sources are presented in Fig. 4. The center of the cross indicates the radio position, and the angular size of the cross hairs is fixed at $20''$, independent of the plate scale of any particular observation.

3.2. Magnitudes

We estimate the photometric accuracy for the optical bands to be on the order of 0.1 magnitude for the brighter sources ($m \lesssim 21$), increasing to ~ 0.4 mag for the faint end of the sample ($m \sim 22.5$). None of the nights were photometric, and most of the sources are not properly exposed for accurate photometry. In case of an empty field (e.g. 1045+019), the optical counterpart must be fainter than the limiting magnitude of the CCD frames. A conservative estimate of this limit is ~ 23 (in any of the bands). The photometry results can be found in the last column of Table 2.

3.3. Spectra and redshifts

For 22 of the 29 sources, low dispersion spectra were taken with the sole objective of assessing redshifts. The typical $\sim 30 \text{ \AA}$ resolution is sufficient to resolve the [O III] 4959/5007 \AA doublet, one of the most prominent emission features in optical spectra of radio galaxies. Furthermore, this resolution is a reasonable trade-off between signal-per-pixel and spectral resolution. The results are listed in Table 3. The spectra with positive line identifications are displayed in Figs. 1 and 2.

The following sources remain without proper redshift determination:

0018+729, 0159+839, 0316+161, 0437-454, 0602+780,
0703+468, 0742+103, 0802+212, 0904+039, 0914+114,
1045+019, 1433-040, 1601-222, 1648+015, 1732+094,
1815-553, 1942+772, 2322-040

4. Comments on selected sources

0018+729 Recently Snellen et al. (1996) listed a redshift for this source of 0.821, based on a single [O II] identification. In our 3600 s spectrum, no such line is seen. We do detect a single faint emission line at 5960 \AA , but this does not agree with the 0.821 redshift. Until a better spectrum becomes available, we consider this source without a reliable redshift determination.

0159+839 Spoelstra et al. (1985) classified this object as 17th mag “stellar” object. Our spectrum does not show any prominent emission lines though, only a possible line partly absorbed by the A-band (around 7600 \AA).

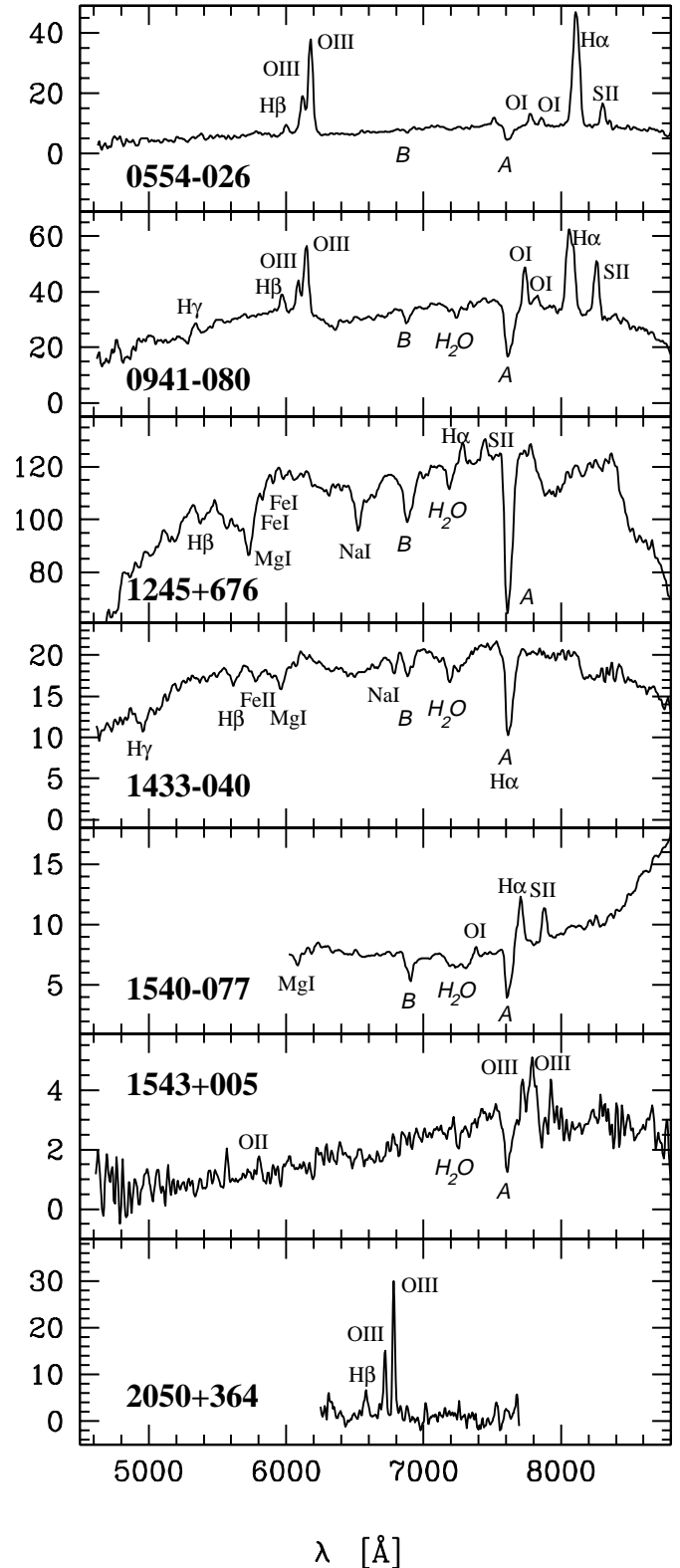


Fig. 1. Optical spectra for the sources with identified lines. Features not related to the source, e.g., the atmospheric absorption bands *A* and *B*, are indicated in italics. Fluxes are in units of $10^{-17} \text{ ergs s}^{-1} \text{ cm}^{-2} \text{ \AA}^{-1}$

Table 2. Positions and magnitudes of identifications

Name	Optical position (2000.0)						R -value	ID	mag ^a
	h	m	s	°	'	"			
0437−454	04	39	00.84	−45	22	22.3	0.3	G	19.0 I
0742+103	07	45	33.17	10	11	15.3	4.4	G	~ 24
0802+212	08	05	38.61	21	06	51.6	0.9	G	22.5 R
0904+039	09	06	40.98	03	42	42.3	0.8	G	22.1 I
1433−040	14	35	40.08	−04	14	54.5	1.3	G	18.3 R
1540−077 ^b	15	43	01.64	−07	57	06.8	0.4	G	17.8 R
1601−222	16	04	01.41	−22	23	42.6	2.9	G	19.3 R
1648+015	16	51	03.72	01	29	21.4	3.9	G	21.4 R
1732+094	17	34	58.42	09	26	59.5	1.1	G	21.3 R
1815−553	18	19	45.40	−55	21	20.4	0.6	G	22.0 V
1942+722	19	41	27.29	72	21	43.7	3.6	G	17.64 ± 0.05 K
2121−014	21	23	39.26	−01	12	34.2	0.9	G	18.18 ± 0.08 K
2128+048	21	30	32.94	05	02	17.3	1.8	G	17.47 ± 0.04 K
2322−040	23	25	10.25	−03	44	47.3	0.6	G	17.46 ± 0.04 K

^a Indicated filters are: Johnson V , I , R , and the near-IR K -band.

^b Some confusion reigned about the exact radio position of this source. The optical position listed here is the correct identification (cf. notes on this object).

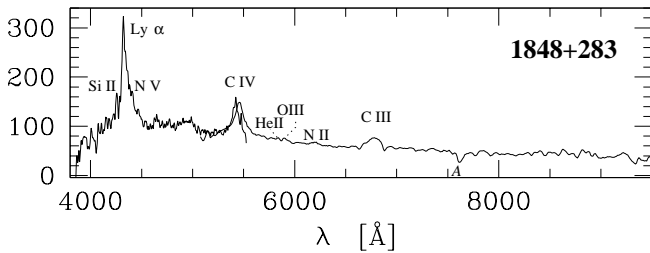


Fig. 2. GPS quasar 1848+283. Note the overlap between the red and blue arms of the spectrograph around C IV. Units and markings are identical to Fig. 1

0316+161 This faint galaxy has long defied a proper redshift assessment, and our 3600 s exposure also proved too shallow.

0437−454 Our optical identification agrees with the one given by Jauncey et al. (1989). Unfortunately, our spectrum does not show any significant features.

0500+019 This source has already been described in Paper I, but Stickel et al. (1996) later suggested the GPS source to be a background quasar, based on a single unidentified emission line at 6543 Å. Our 1995 redshift measurement ($z = 0.583$) would therefore be of an intervening galaxy. However, we do not see any evidence of this 6543 Å line in our spectrum, nor does our Hubble Space Telescope NICMOS J and K band data show a hint of this quasar—galaxy superposition (cf. De Vries 1999). The recent H I absorption redshift of 0.58472 (Carilli et al. 1998) is therefore *intrinsic* and not due to an intervening absorber, as Stickel et al. suggest.

0507+179 We tentatively confirm the $z = 0.416$ redshift based on the better signal-to-noise spectrum of

Perlman et al. (1998). In our 3600 s exposure faint emission features may be identified with [O II] at 5263 Å, and [O III] at 7107 Å, resulting in redshifts of 0.412 and 0.419 respectively. Without the Perlman et al. spectrum these identifications would be *very* tentative though. This source is most likely a BL Lac object, with a foreshortened radio structure due to the orientation in the sky, and not an intrinsically small radio source like the GPS.

0554−026 The radio position given by Spoelstra et al. (1985) for this object was accurate only within 10 arcsec and close to a stellar object. We initially used this position, thereby obtaining a spectrum of this star. At a later stage, we discovered that the radio position given by McEwan et al. (1975) corresponds with the galaxy approximately 10 arcsec to the northeast of the star (cf. Paper I). During the 1996 Kitt Peak run we obtained a good quality emission spectrum for this galaxy (cf. Fig. 1), and were able to determine its 0.235 redshift.

0602+780 Spoelstra et al. (1985) listed the identification as an empty field, but Stanghellini et al. (1993) detected a very faint object close to the radio position. Unfortunately, this object proved too faint to produce a significant signal on a 4 m-class telescope within an hour.

0703+468 Like 0602+780, this source is taken from the Spoelstra et al. (1985) radio spectral sample. Stanghellini et al. (1993) identified this source with a 23rd mag object. Our 3600 s spectrum proved inadequate.

0742+103 After combining 600 s exposures in R ($\times 2$), V , and I band, creating a wide passband 2400 s exposure, we were just able to detect an optical counterpart to the radio source. Its brightness is on the order of 24th magnitude. This identification agrees with the Fugmann

Table 3. Redshifts + line identifications

Source	Line	Wavelength (Å)	Redshift	Mean	Remarks
0554–026	H β 4861	5999	0.234		
	[O III] 4959	6120	0.234		
	[O III] 5007	6178	0.234		
	[O I] 6300	7778	0.235		
	[O I] 6364	7858	0.235		
	H α 6563+[N II] 6584	8110	0.234		
0941–080	[S II] 6717/6731	8304	0.235	0.235	
	H β 4861	5971	0.228		
	[O III] 4959	6088	0.228		
	[O III] 5007	6146	0.227		
	[O I] 6300	7737	0.228		
	[O I] 6364	7831	0.231		
1245+676	H α 6563+[N II] 6584	8068	0.227		
	[S II] 6717/6731	8258	0.228	0.228	
	H β 4861	5384	0.1076		absorption
	Mg I 5175	5726	0.1065		absorption
	Fe I 5270	5827	0.1065		absorption
	Fe I 5328	5905	0.1083		absorption
1433–040 ^a	Na I 5893	6524	0.1071		absorption
	H α 6563+[N II] 6584	7282	0.1078		
	[S II] 6717/6731	7446	0.1074	0.1073	
	H β 4861	5616	0.1553		absorption
	Fe II 5018	5781	0.1521		absorption
	Mg I 5175	5961	0.1518		absorption
1540–077	Na I 5898	6786	0.1506		absorption
	H α 6563+[N II] 6584			0.152	blends with A-band
	Mg I 5175	6081	0.175		absorption
	[O I] 6300	7382	0.172		
	H α 6563+[N II] 6584	7708	0.173		
	[S II] 6717/6731	7879	0.172	0.172	
1543+005	[O II] 3727	5802	0.557		
	[O III] 4959	7712	0.555		
	[O III] 5007	7789	0.556	0.556	
1848+283	[O III] 5007	7789	0.556	0.556	
	Si II 1194	4255	2.563		
	Ly α 1216	4322	2.554		
	N V 1240	4406	2.554		
	C IV 1549	5425	2.502		blue arm
	C IV 1549	5457	2.523		red arm
	He II 1640	5836	2.559		
	O III] 1663	5897	2.546		
	[N II] 1750	6201	2.543		
	C III] 1909	6776	2.550	2.544	
2050+364	H β 4861	6580	0.354		
	[O III] 4959	6718	0.355		
	[O III] 5007	6783	0.355	0.355	

^a Not the GPS source, see notes on object.

et al. (1988) identification. Larger telescopes are needed to properly assess the source morphology and redshift.

0802+212 The optical counterpart is the faint patch of emission due south of the brighter point source. It is accurately centered on the radio position. The spectrum proved featureless, however.

0904+039 The radio source is identified with a 22nd mag object, which appears slightly extended in our *I* band

image. This source seems to reside in a small group of objects (presumably galaxies).

0914+114 The source spectrum features one bright emission line, which initially was interpreted by us as H α at $z = 0.178$. Subsequent scrutiny did cast some doubt on this, and in a higher resolution spectrum taken in 1998 we do not find any evidence for this emission feature.

Table 4. Emission line fluxes

Source	Redshift	Line	Flux ^a	EqW ^b	FWHM (obs) ^c	FWHM (int) ^d
0554–026	0.235	H β 4861	11.0	17	33	11
		[O III] 4959	54.7	81	40	21
		[O III] 5007	126.0	181	34	13
		[O I] 6300	9.9	9	39	20
		[O I] 6363	4.6	5	30	–
		H α + [N II]	216.0	229	57	39
		[S II] 6717+6731	25.8	31	34	13
0941–080	0.228	H γ 4340	13.5	7	43	25
		H β 4861	28.5	9	42	24
		[O III] 4959	49.9	17	36 ^e	16
		[O III] 5007	112.0	33	37 ^e	18
		[O I] 6300	43.7	13	34 ^e	13
		[O I] 6363	10.2	3	41 ^e	23
		H α + [N II]	187.0	60	71 ^e	52
1540–077	0.172	[S II] 6717+6731	83.4	27	44 ^e	26
		[O I] 6300	1.6	2	27 ^e	15
		H α + [N II]	19.9	21	41 ^e	31
		[S II] 6717+6731	9.8	12	38 ^e	27
		[O II] 3727	1.3	12 ^e	32 ^e	7
		[O III] 4959	2.8	9 ^e	40 ^f	17
		[O III] 5007	8.1	22 ^e	73 ^f	43
1848+283	2.544	Ly α ^g 1216	1700	203	47	13
		C IV 1549	1000	150	75	20
		C III] 1909	350	60	148	41

^a In units of 10^{-16} ergs s⁻¹ cm⁻².

^b Measured equivalent width [Å].

^c Measured FWHM [Å].

^d FWHM [Å] after instrumental and redshift corrections. Instrumental resolution is taken to be 30 Å for CRYOCAM and 20 Å for EFOSC1, based on skylines.

^e After smoothing spectrum with a 3 pixel boxcar.

^f After smoothing spectrum with a 5 pixel boxcar.

^g Line flux includes contributions by Si II 1194, Si III 1206, and N V 1240.

0941–080 This interacting binary source (cf. De Vries 1999) has a prominent emission line spectrum. The redshift is 0.228, based on 7 identified spectral features. The GPS source is associated with the northern galaxy.

1045+019 Gopal-Krishna et al. (1983) list this as an empty field, and after 600 s in R we have to agree. The radio spectrum of the source appears rather flat (O’Dea et al. 1990), so this might not even be a true GPS source. Stanghellini et al. (1990) detected faint extended radio emission associated with this source, strengthening its non-GPS nature.

1245+676 Our redshift determination of $z = 0.1073$ agrees very well with the recent one by Falco et al. (1998): 0.1073 ± 0.0002 .

1433–040 This source is identified in the NED database as 4C –04.51, which is incorrect. The correct radio position of 4C –04.51 is $14^{\text{h}}35^{\text{m}}49^{\text{s}}.05 -5^{\circ}16'12''.3$ (J2000), based on the NRAO/VLA Sky Survey (NVSS) catalog. The position listed in Table 1 for 1433–040 is also from the NVSS catalog, which we feel is more accurate than the Texas 365 MHz position (Douglas

et al. 1996). We obtained a spectrum for the object close to the Spoelstra et al. (1985) position, which is not the correct radio position either ($14^{\text{h}}35^{\text{m}}39^{\text{s}}.83 -4^{\circ}13'46''.4$). The redshift listed in Table 3 is therefore of an unrelated field galaxy.

1540–077 Our redshift determination for this source is 0.172, based on 4 identified lines.

1543+005 The literature redshift of 0.55 is an estimate given in Heckman et al. (1994). Incidentally, it turned out to be an accurate estimate; we measured a redshift of 0.556.

1601–222 Even despite the large R -value of ~ 3 , we feel confident the (large) galaxy seen close to the radio position is indeed the host. Actually, the best radio position is within the optical extent of the galaxy. Our identification of this source confirms the earlier identification of Drinkwater et al. (1997). Our spectrum is featureless.

1648+015 The source spectrum is featureless. The optical identification agrees with Drinkwater et al. (1997).

1732+094 This object is rather faint ($\sim 21^{\text{st}}$ mag), and in close proximity to a very bright star, making

it hard to assess its redshift. Our spectrum proved too shallow.

1815–553 The spectral range of 5000 – 10000 Å is probably too red for this object, as it seems to be very blue. It appears significantly brighter on the IIIa-J plate of Jauncey et al. (1989). Our (red) spectrum is featureless. This object, based on its colors, is probably a quasar.

1848+283 The spectrum of this quasar was taken with FOS on the INT, which had a blue and a red arm of the spectrometer. Unfortunately, the C IV emission line landed on either edge of the spectral arm. Therefore, the small overlap region does not quite match up (cf. Fig. 2).

1942+772 This source is from the fainter (in radio luminosity) GPS sample of Snellen et al. (1998a). Our K band image provides a definite determination of the optical counterpart and its overall morphology, something not clear in the images presented by Snellen et al. (1998a).

2121–014 This source has been imaged by us before (Paper I), where we barely detected it in the i band. In the image presented here, its double structure stands out for the first time. It is not clear whether the radio source resides in the eastern or western component. Both are presumably individual galaxies, engaged in close interaction.

2128+048 Our identification agrees with the initial one made by Biretta et al. (1985). They already noted its redness ($R-I \approx 1.5$), something which is confirmed here by its relative brightness in K .

2322–040 Our image provides a larger field of view than the identification frame of Stanghellini et al. (1993). The galaxy appears to be a regular elliptical, possibly a member of a small group of galaxies.

5. Colors of high redshift radio galaxies

Based on our previous work on GPS host galaxies in the near infrared (De Vries et al. 1998a, 1998b), we know their galaxy colors to be consistent with those predicted by stellar synthesis models (e.g., Bruzual & Charlot 1993). Since we are imaging GPS galaxies around a redshift of 1, the expected $R-K$ color is around 5 to 6. Indeed, the sources 2121–014 and 2128+048 both have an $R-K$ color of ~ 5.7 and measured redshifts of 1.16 and 0.99 respectively. These points lie close to the passive evolutionary track (cf. Fig. 3), however, in the case of 2121–014 with its large uncertainty in the published R band magnitude (~ 1 mag, Snellen et al. 1996) this may be coincidental. Based on the $R-K$ colors of the two other sources, ~ 5.4 , and ~ 6.0 for 1942+772 and 2322–040 respectively, their most likely position in the plot is indicated by the overplotted box. The implicit assumption here is that the sources have colors matching those of an old, passively evolving galaxy, which was found to be the case for our near-IR and NICMOS samples (De Vries 1999).

Judging by their position in the plot, these sources are probably going to be among the highest redshift GPS

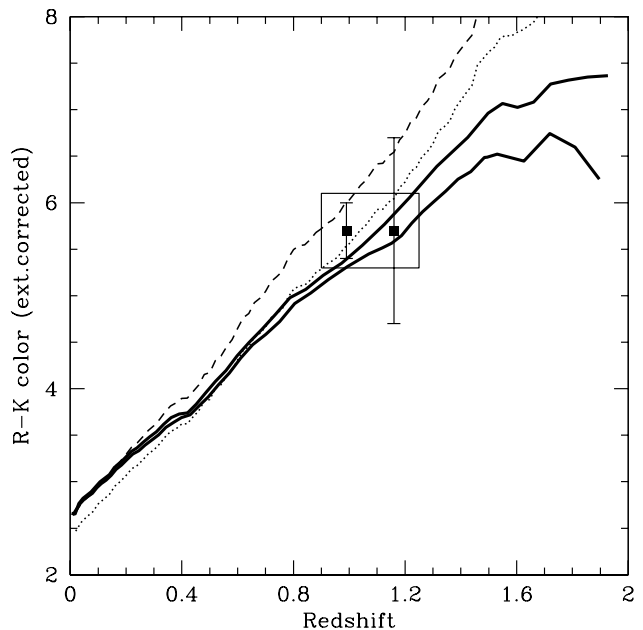


Fig. 3. Predicted galaxy colors based on stellar synthesis models. Dashed lines indicate a fixed mean stellar age, 10 Gyrs for the top track, 5 Gyrs for the bottom one. The solid lines are for passively evolving galaxies, with an initial burst of star formation at $z = 6$ (top) and $z = 3$ (bottom). All tracks are computed assuming a mean solar metallicity. The points are $R-K$ colors for 2128+048 and 2121–014 (left and right data point, respectively). The overplotted box indicates the range where the data points of 1942+772 and 2322–040, both without redshift information, are most likely to land on the plot

galaxies currently known. The remaining empty fields (e.g. 0008–421, cf. Paper I) are presumably at higher redshift still. This extension of the redshift baseline for our GPS sample is much needed to distinguish for instance between the various evolutionary models. Note how in Fig. 3 the tracks start to diverge around the $z = 1$ mark. Currently 2121–014 is among one of the very few $z > 1$ GPS galaxies, and not very well constrained in R magnitude. Obviously moving to large aperture telescopes and into the near-IR in order to minimize possible non-stellar color contamination (e.g. De Vries et al. 1999), will improve significantly on the yield of color-redshift plots like these.

The published images for these sources are not very deep, and often barely detect the host galaxy (cf. notes on individual objects). Our Keck images not only unambiguously show the galaxies, but also provide morphological information. The source 2121–014, for instance, has a double structure (cf. Fig. 5) reminiscent of two closely interacting galaxies.

To summarize, in order to complete the identification and redshift determination of the faint end of our GPS sample, we need to use facilities with comparable collecting areas, i.e., 8 meter class telescopes. In an

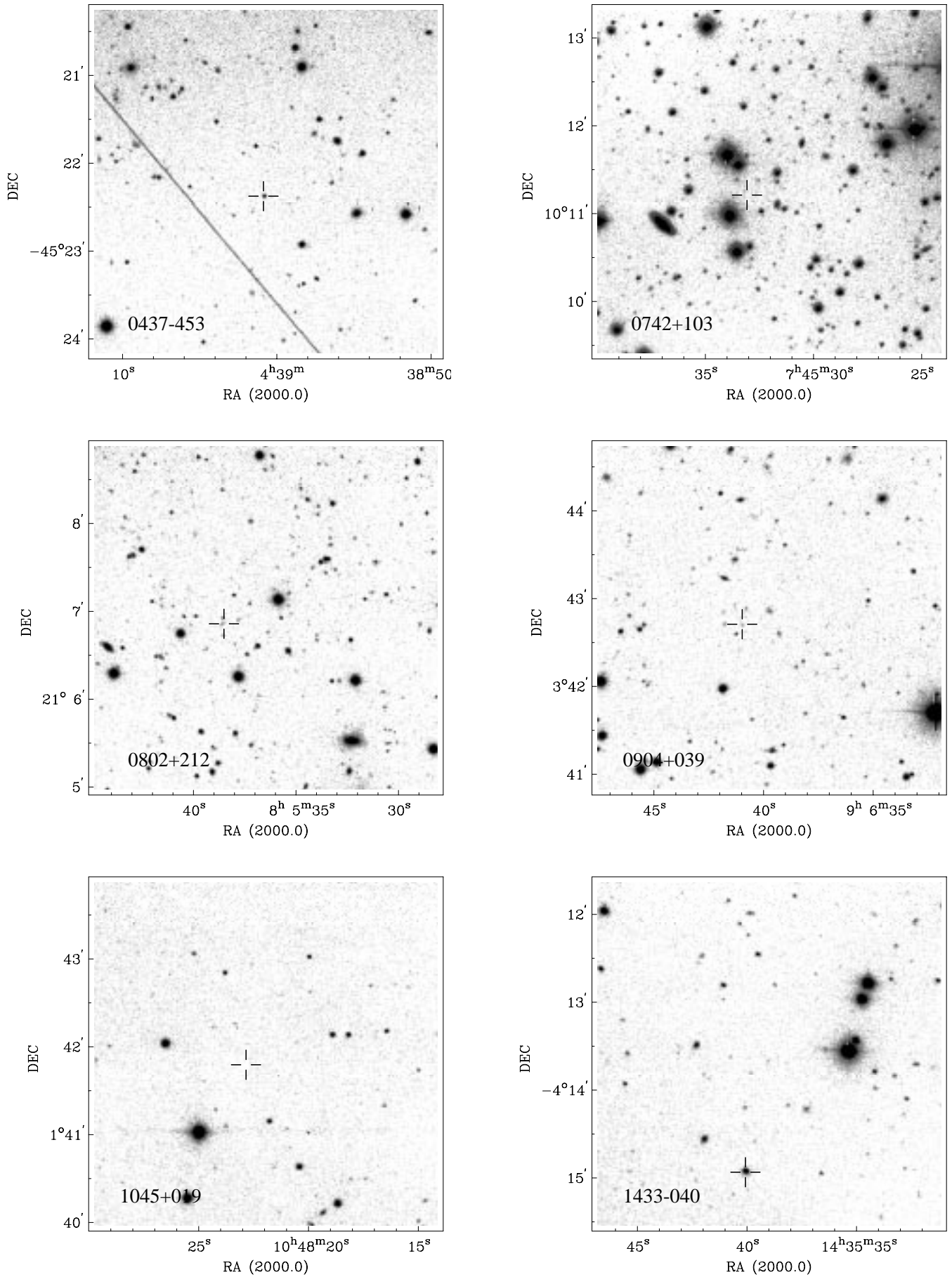


Fig. 4. Finding charts for the GPS sources, with accurate radio positions overplotted

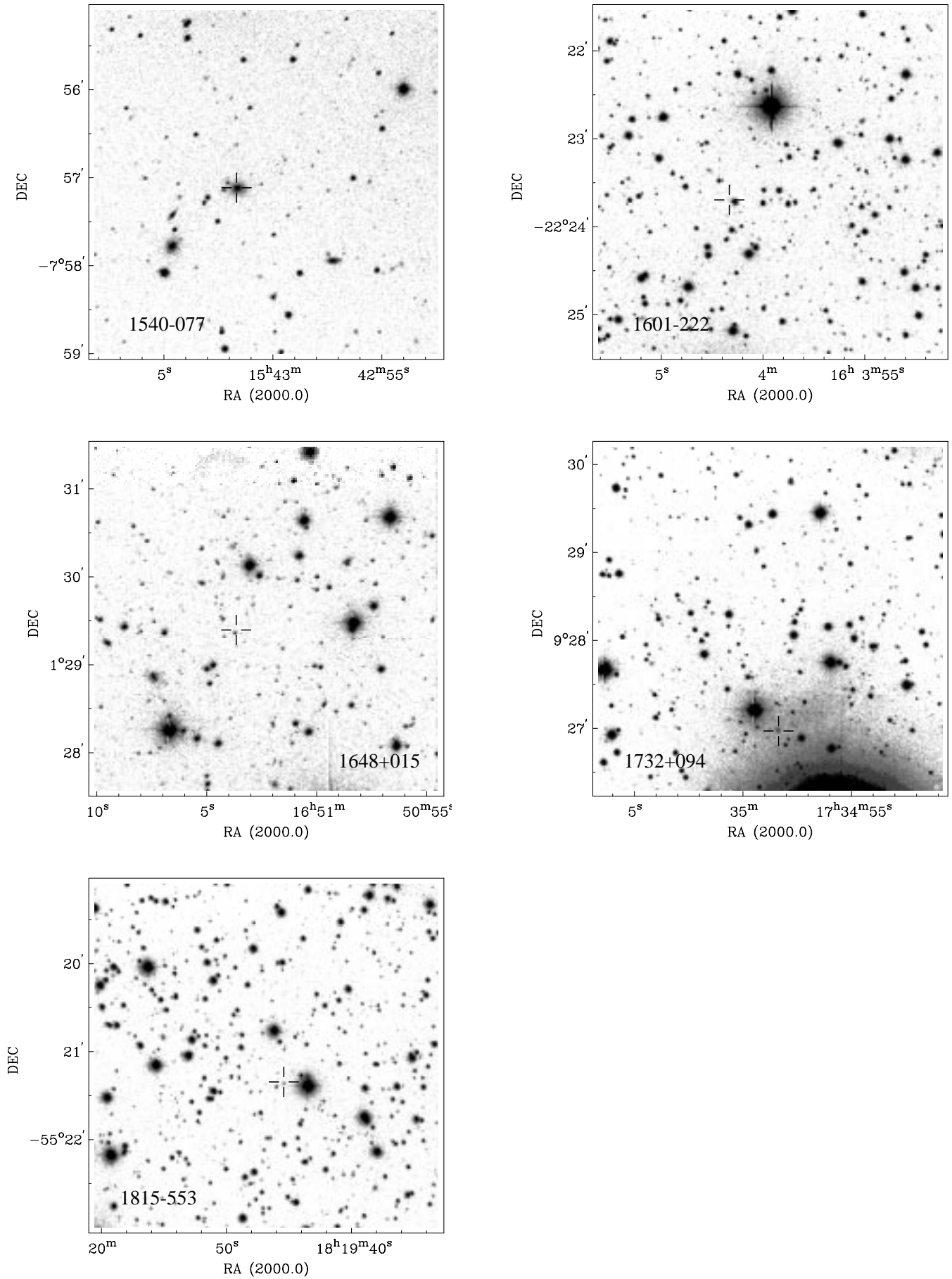


Fig. 4. continued

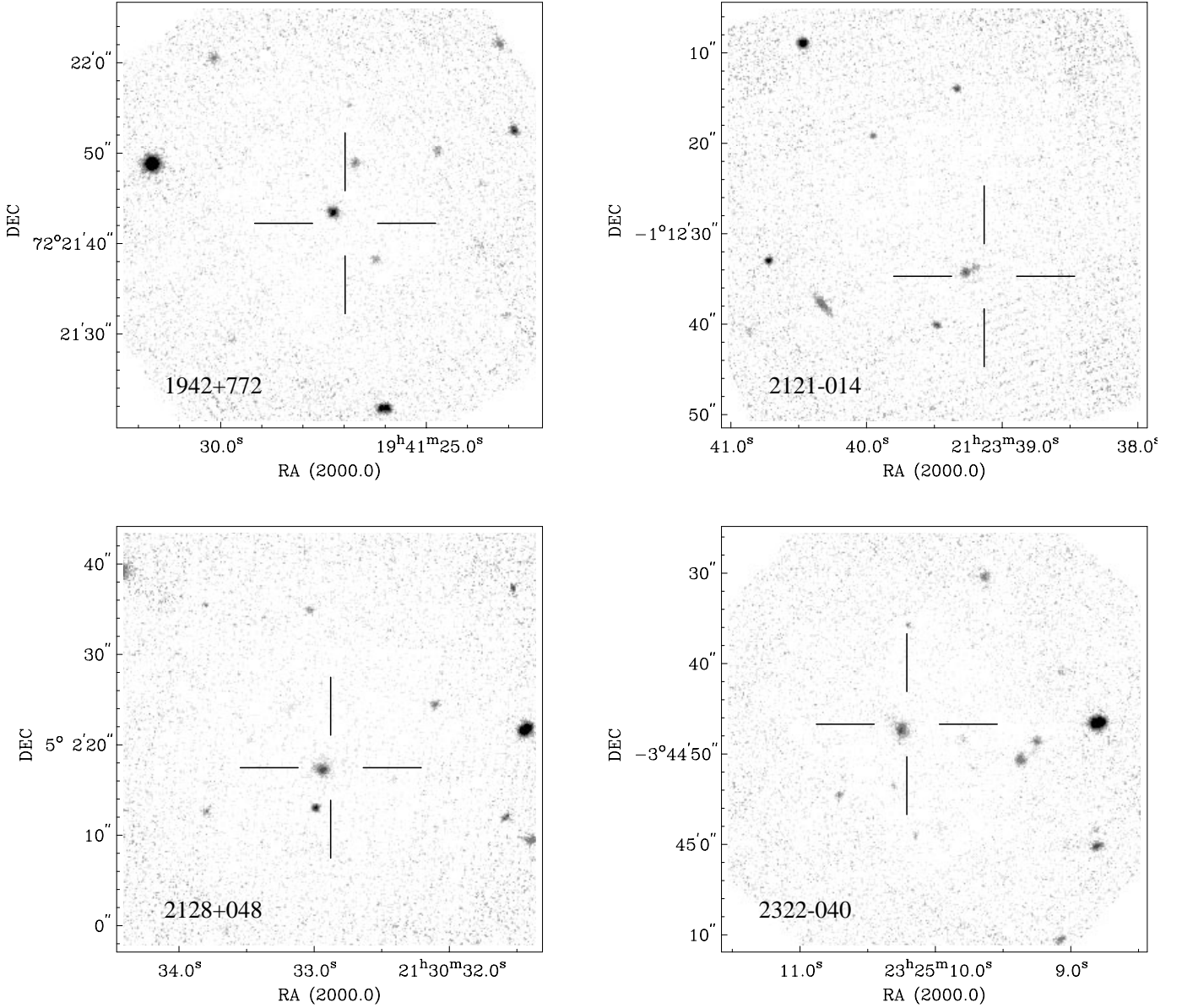


Fig. 5. Keck K band images of 4 optically faint GPS galaxies

upcoming paper we will report on results from our first VLT program.

6. Summary

We have presented deep optical and near-IR images of 15 GPS sources with previously unknown optical counterparts or undetermined morphologies. New or revised identifications and magnitudes have been obtained for 5 GPS galaxies. In total, spectra were obtained for 22 sources, resulting in 7 new GPS redshift determinations. The remaining empty fields and sources without proper redshifts are most likely intermediate redshift galaxies, based on their optical faintness and in some cases large $R - K$ col-

ors. Eight meter class telescopes are needed to complete identification and redshift determination of 1 Jy class GPS radio sources.

Acknowledgements. The authors like to thank Arjun Dey for his spectroscopic observations of 2050+364.

References

- Begelman M.C., 1998, in: “The Most Distant Radio Galaxies”, proceedings of the KNAW colloquium Amsterdam, Röttgering H.J.A., Best P., Lehnert M.D. (eds.). Kluwer (in press) (astro-ph/9712107)
- Biretta J.A., Schneider D.P., Gunn J.E., 1985, AJ 90, 2508
- Bruzual A.G., Charlot S., 1993, ApJ 405, 538

- Carilli C.L., Menten K.M., Reid M.J., Rupen M.P., Yun Min Su, 1998, *ApJ* 494, 175
- de Ruiter H.R., Willis A.G., Arp H.C., 1977, *A&AS* 28, 211
- de Vries W.H., 1999, Ph.D. Thesis, University of Groningen, The Netherlands
- de Vries W.H., Barthel P.D., Hes R., 1995, *A&AS* 114, 259 (Paper I)
- de Vries W.H., Barthel P.D., O'Dea C.P., 1997, *A&A* 321, 105
- de Vries W.H., O'Dea C.P., Perlman E., et al., 1998a, *ApJ* 503, 138
- de Vries W.H., O'Dea C.P., Baum S.A., et al., 1998b, *ApJ* 503, 156
- de Vries W.H., O'Dea C.P., Baum S.A., Barthel P.D., 1999, *ApJ* 526, 27
- Douglas J.N., Bash F.N., Bozayan F.A., Torrence G.W., Wolfe C., 1996, *AJ* 111, 1945
- De Young D.S., 1997, *ApJ* 490, L55
- Drinkwater M.J., Webster R.L., Francis P.J., et al., 1997, *MNRAS* 284, 85
- Falco E.E., Kochanek C.S., Muñoz J.A., 1998, *ApJ* 494, 47
- Fanti C., Fanti R., Dallacasa D., et al., 1995, *A&A* 302, 317
- Fugmann W., Meisenheimer K., Röser H.-J., 1988, *A&AS* 75, 173
- Gopal-Krishna, Patnaik A.R., Steppe H., 1983, *A&A* 123, 107
- Heckman T.M., O'Dea C.P., Baum S.A., Laurikainen E., 1994, *ApJ* 428, 65
- Jauncey D.L., Savage A., Morabito D.D., et al., 1989, *AJ* 98, 54
- Johnston K.J., Fey A.L., Zacharias N., et al., 1995, *AJ* 110, 880
- Ma C., Arias E.F., Eubanks T.M., 1998, *AJ* 116, 516
- Matthews K., Soifer B.T., 1994, in "Infrared Astronomy with Arrays", McLean I. (ed.). Dordrecht: Kluwer, p. 239
- McEwan N.J., Browne I.W.A., Crowther J.H., 1975, *MemRAS* 80, 1
- O'Dea C.P., 1998, *PASP* 110, 493
- O'Dea C.P., Baum S.A., Stanghellini C., et al., 1990, *A&AS* 84, 549
- O'Dea C.P., Baum S.A., Stanghellini C., 1991, *ApJ* 380, 66
- O'Dea C.P., Stanghellini C., Baum S.A., Charlot S., 1996, *ApJ* 470, 806
- O'Dea C.P., Baum S.A., 1997, *AJ* 113, 148
- Patnaik A.R., Browne I.W.A., Wilkinson P.N., Wrobel J.M., 1992, *MNRAS* 254, 655
- Perley R.A., 1982, *AJ* 87, 859
- Perlman E.S., Padovani P., Giommi P., et al., 1998, *AJ* 115, 1253
- Readhead A.C.S., Taylor G.B., Xu W., et al., 1996a, *ApJ* 460, 612
- Readhead A.C.S., Taylor G.B., Pearson T.J., Wilkinson P.N., 1996b, *ApJ* 460, 634
- Snellen I.A.G., Bremer M.N., Schilizzi R.T., Miley G.K., van Ojik R., 1996, *MNRAS* 279, 1294
- Snellen I.A.G., Schilizzi R.T., Bremer M.N., et al., 1998a, *MNRAS* 301, 985
- Snellen I.A.G., Schilizzi R.T., de Bruyn A.G., et al., 1998b, *A&AS* 131, 435
- Spoelstra T.A.T., Patnaik A.R., Gopal-Krishna, 1985, *A&A* 152, 38
- Stanghellini C., Baum S.A., O'Dea C.P., Morris G.B., 1990, *A&A* 233, 379
- Stanghellini C., O'Dea C.P., Baum S.A., Laurikainen E., 1993, *ApJS* 88, 1
- Stickel M., Rieke M.J., Rieke G.H., Kühr H., 1996, *A&A* 306, 49
- Urry C.M., Padovani P., 1995, *PASP* 107, 803
- White G.L., 1992, *Proc. Astron. Soc. Australia* 10, 140
- Wright A., Otrupcek R., 1990, Parkes Catalog, Australia Telescope National Facility